


Article

Size-Dependent Microplastic Fragmentation Model

Vicente Pérez-Muñuzuri 

CRETUS, Group of Nonlinear Physics, University of Santiago de Compostela,
E-15782 Santiago de Compostela, Spain; vicente.perez.munuzuri@usc.es

Abstract: Plastic fragmentation alters the size distribution of plastic waste in aquatic habitats, which is accelerated by mechanical stress and weathering degradation processes. Microplastic pieces constitute the vast bulk of plastic pollution in terms of quantity. Their size distribution has been shown to follow a power-law for larger fragments. This work introduces a novel model inspired by raindrop formation, incorporating local oceanographic processes and fragment size, aiming to improve the understanding and prediction of plastic fragmentation in marine environments. Particles can fragment when they reach a certain size, or when shear forces become too strong. Plastic aging's effect on size distribution is also investigated.

Keywords: microplastics; fragmentation model; degradation; size distribution

1. Introduction

Plastic pollution is a worldwide environmental issue that has received substantial attention due to its harmful effects on ecosystems and human health. According to [1,2], the global plastic load on the open ocean surface is estimated to be in the tens of thousands of tons, which is significantly lower than expected. Resolving the fate of the missing plastic debris is critical for determining the nature and significance of plastic pollution's effects in the oceans. Fast fragmentation into nano- and micro-scale plastics may be behind this phenomenon [3]. Based on field studies conducted in the global oceans, microplastic fragments account for the majority of plastic pollution in terms of abundance [2,4–7]. Understanding and anticipating the fragmentation process is essential for assessing the environmental impact of plastic trash. Fragmentation not only enhances the quantity and distribution of plastic particles, but it also boosts their bioavailability, allowing them to be absorbed by a wide range of species at all trophic levels. These particles can collect and concentrate hazardous pollutants, posing substantial risks to both animal and human health through trophic transmission [8].

The fragmentation process influences plastic transport, because smaller fragments have a higher surface area than their volume, resulting in increased degradation rates and decreased buoyancy. Removal mechanisms for microplastics include ingestion by planktivorous animals and ballasting by biofouling, which results in the movement of micro- and nanoplastics from the surface to the water, sediment, or column [4,8–10].

Despite numerous studies on plastic pollution, there is still a significant gap in our ability to accurately model plastic fragmentation [11–13]. The existing research has primarily relied on empirical observations and laboratory experimentation from the materials science point of view; experiments on the brittle and crack fragmentation of objects with different materials and shapes [14–17], the impact of single particles in a pneumatic conveying system [18], the impact of polypropylene particles of spherical shape against a hard wall [19], the fragmentation of flexible and brittle fibers in a turbulent flow [20], photo aging and fragmentation of food packaging materials in seawater [21], and degradation and later fragmentation of plastics in the environment [22], among many others references published during last decades.



Citation: Pérez-Muñuzuri, V.
Size-Dependent Microplastic
Fragmentation Model. *J. Mar. Sci.
Eng.* **2024**, *12*, 1213. [https://doi.org/
10.3390/jmse12071213](https://doi.org/10.3390/jmse12071213)

Academic Editor: Jean-Marc
Guarini

Received: 13 June 2024
Revised: 6 July 2024
Accepted: 17 July 2024
Published: 19 July 2024



Copyright: © 2024 by the author.
Licensee MDPI, Basel, Switzerland.
This article is an open access article
distributed under the terms and
conditions of the Creative Commons
Attribution (CC BY) license ([https://
creativecommons.org/licenses/by/
4.0/](https://creativecommons.org/licenses/by/4.0/)).

All of these laboratory experiments and ocean observations share a common particle size distribution (PSD), which specifies the abundance or mass of particles for various size classes. PSD data often shows a maximum for small pieces and a power law for bigger fragments [2,4,7,23–25]. Experiments on the fragmentation of plastic materials demonstrate that the size distribution of pieces produced by a plastic object follows a fractal process. Numerical models rely on Turcotte’s 1986 work [26], which showed that the scale-invariance of the fragmentation process, whether caused by weathering, explosions, or impacts, produces such a power law. Statistical models of brittle fragmentation have been developed to study fragment size distribution (see [27] for a review). More recently, other deterministic models have been proposed to reproduce this power-law distribution [7,28–30]. These models assume that a larger component of size r_i divides into a smaller one $r_{i+1} = pr_i$ with some probability $p < 1$. The division process is repeated over time in a cascading fashion, satisfying a fractal distribution condition over a wide range of scales, resulting in a geometric progression of fragment sizes yielding the power-law

$$N(r) \propto r^{-\alpha} \tag{1}$$

where N is the abundance, r is the particle characteristic size, and α is the power law slope. These models do not account for differences in fragmentation probability based on fragment size, nor do they take into account flow features that may influence fragmentation in certain regions of the ocean more than others. Aoki and Furue (2021) [31] proposed a model that takes into account the size of the plastic and the energy required for fragmentation, under two assumptions: fragmentation into smaller pieces requires more energy, and the occurrence probability of the energy decreases exponentially as energy values rise.

Marine litter plastic fragmentation is typically ignored in Lagrangian transport models due to a lack of realistic models and/or numerical issues coping with the rapid growth of particle numbers (dynamic memory allocation). Some Lagrangian models address the microplastics input contribution from different sizes, assuming their number decreases with size, following the prior power function [13,24,32].

This work provides a novel model for plastic fragmentation that addresses these issues by drawing on the principles that underpin raindrop generation in clouds [33,34]. The model incorporates the dependence on local oceanographic process, plastic aging and fragment size as criteria for fragmentation that were not previously addressed.

2. Numerical Model

We assume that plastic items do not affect the flow. Thus, their evolution is identical to that of passive point-like particles, and they follow the flow streamlines. Furthermore, the plastics breakup occurs instantaneously when subjected to a hydrodynamic stress that exceeds a critical value [33,34]. Thus, fragmentation takes place when the shear force acting on the particle of mass m exceeds a critical value

$$S_{crit} = \frac{p}{\gamma} \cdot \frac{r_0}{r} \tag{2}$$

where $p \in [0, 1)$ is a uniformly distributed random number, γ accounts for the effects of plastic weathering and specific characteristics of the object (density, crystallinity, brittleness, etc.) that may influence its fragmentation, r_0 is the largest particle size, and $r \leq r_0$ is the actual size of the particle. The threshold shear becomes smaller for larger particles, since larger particles are more susceptible to turbulent shear stresses. Including the term r_0/r in Equation (2) aligns with experiments, demonstrating that smaller pieces are less prone to break [20].

The shear force is calculated as

$$S = (2S_{ij}S_{ij})^{1/2} \quad S_{ij} = \frac{1}{2} \left(\frac{\partial u_i}{\partial x_j} + \frac{\partial u_j}{\partial x_i} \right) \tag{3}$$

where u_i are the flow velocity components at the particle position x_i . For simplicity, in this paper, we use a two-dimensional sinusoidal-shear flow model [35] depicted in Appendix A. Dimensionless time units (t.u.) and space units (s.u.) are used throughout.

If the shear force, calculated at the particles position, exceeds the threshold value given by Equation (2), the particle of mass m is divided into N_{pieces} smaller pieces, with masses $m_i = p_i m$, $\sum_i p_i = 1$, and $p_i \in [0, 1)$ being uniform random numbers. The centers of the pieces are located at a distance equal to the sum of their radii from the initial position of the fractured particle. We consider inelastic collisions between particles as they are advected by the flow.

For each particle, the splitting condition (2) is checked at a frequency rate f_{frag} . New primary particles are added randomly into the model at a frequency rate f_{input} . Two different sets of primary particles entering the system were analyzed: (i) all of them having the same radius $r_0 = 5$ (s.u.), or (ii) their radii being selected uniformly randomly within the interval $r_0 \in [10^{-3}, 5]$ (s.u.).

3. Results

The fragmentation of particles leads to an exponential increase in the number of particles into the system, as shown in Figure 1. Note that as time evolves, equal size primary particles entering the system and older fragments break continuously if the shear force exceeds the critical value given by Equation (2). Figure 2 shows the steady-state histogram of the particle distribution as a function of the radius for two different values of γ . The particle distribution exhibits a peak with a long tail towards larger sizes that gradually approaches zero. The effect of randomness p is to broaden the dispersion function. All distributions analyzed in this paper show a scaling form that follows Equation (1), as is typically observed in the ocean plastic distributions [2,4] and in shear-fragmentation experiments [20,36]. To estimate the power-law slope α , we maximized a log-likelihood function [37], as fitting straight lines on log-log plots may induce large biases.

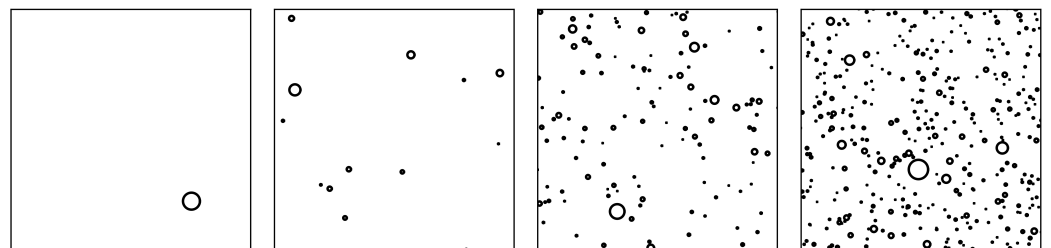


Figure 1. Time evolution of particles in the model. Equal-sized particles entering the systems fragment if the shear force at the particles position exceeds a critical value (2). Panels show a zoom of the model grid at constant intervals of time. Set of parameters: $V_{max} = 1.4$, $T = 10$, $f_{frag} = 5 \cdot 10^{-4}$, $f_{input} = 10^{-2}$, $N_{pieces} = 2$, and $\gamma = 0.5$.

To determine the influence of the plastic degradation γ on the particle size distribution, the slope $\alpha(t)$ and the average particle radius $\langle r(t) \rangle = \sum_r r N_r(t) / \sum_r N_r(t)$ were computed as a function of time (see Figure S1 in the Supplementary Materials). Figure 3 shows the asymptotic average slope α and particle size $\langle r \rangle$ for different values of γ . The stationary values of α and $\langle r \rangle$ decrease with increasing degradation γ as the shear threshold diminishes and favors fragmentation of particles with smaller sizes, as shown in the size distribution (Figure 2). Note that, for equal size primary particles entering the system, the slope α is smaller than for random size particles, whereas the opposite occurs for the mean radius. As the number of larger particles grows, the size distribution shifts to greater values of the radius. Similar results were achieved (see Figure S2 in the Supplementary Materials) by increasing the number of fragments N_{pieces} a particle splits into, reinforcing the meaning of γ as the plastic’s degradation or aging.

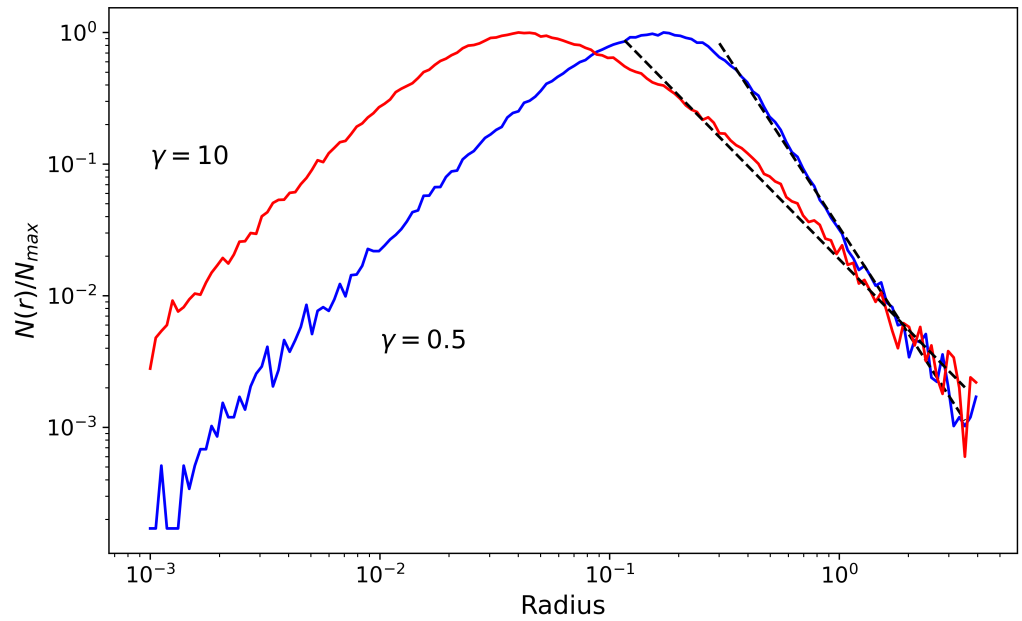


Figure 2. Histogram of the particle size distribution for two values of γ . Equal size particles are considered to enter periodically into the system. Dashed lines correspond to fittings to Equation (1). Set of parameters as in Figure 1.

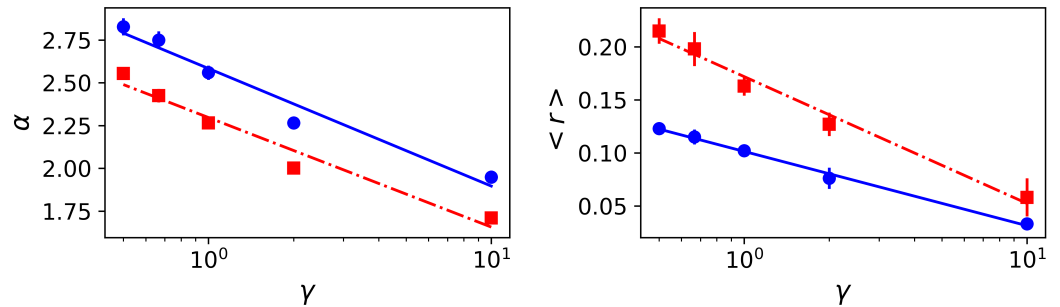


Figure 3. Dependence of the power law slope α and the mean radius $\langle r \rangle$ as a function of the degradation γ for two sets of primary particles entering the system; constant (blue solid line) and random (red dashed line) size. Error bars correspond to different noise realizations for the particles entering the system. Set of parameters as in Figure 1.

Power-law slopes can be compared to data from observations. Table 1 shows the slopes derived from data on the abundance of microplastics as a function of plastic size for observations made in various parts of the world. Modeled values of α are slightly higher than observed values. We used a simple 2D flow model that does not simulate realistic ocean conditions, making it difficult to compare the two types of data. Furthermore, the size distributions shown in Figure S3 in the Supplementary Materials include all types of plastics within the water column, regardless of shape or characteristics. Our model may reproduce similar power-law behaviors, increasing γ , and increasing plastic degradation and/or the ability to break into multiple pieces. This favors fragmentation, and leads to smaller values of α , closer to what is observed.

The last important parameters that typically vary a lot in natural systems are the frequency rates of fragmentation f_{frag} and number of primary particles entering the model f_{input} . Thus, for example, the first one could be related to the influence of tides and waves on plastics hitting rocky shores, whilst the second one corresponds to the rate at which plastics are dumped into the ocean from rivers or the coast. Figure 4 shows the stationary values of α and $\langle r \rangle$ as a function of f_{input} / f_{frag} . Increasing f_{frag} (left of the images) increases

particle fragmentation, especially for larger particles, shifting the size distribution to smaller radius values.

Table 1. Power law slopes α obtained for different domains from observations in the Mediterranean Sea during the MEDSEA campaign in 2013 [38], around the globe during the Malaspina 2010 Circumnavigation [4], and around the Balearic Islands [39]. See their original papers for the detailed locations, and Figure S3 in the Supplementary Materials for a combined graph of abundance versus plastic size for all three cases.

Domain	α
Mediterranean Sea	1.45 ± 0.03
Around Globe	1.84 ± 0.08
Balearic Islands	2.12 ± 0.11

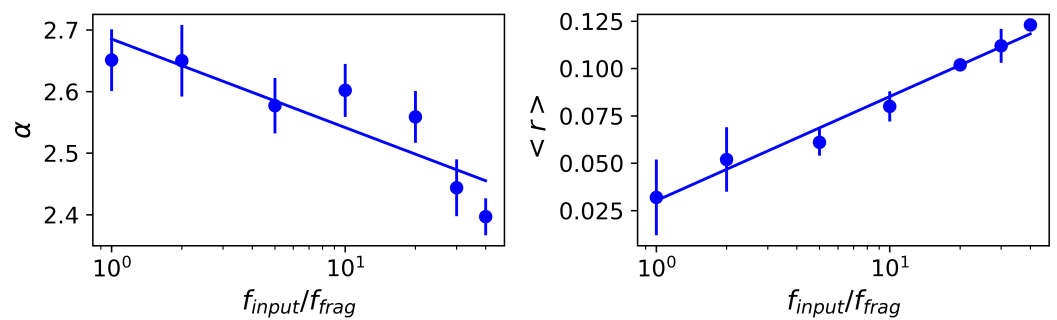


Figure 4. Dependence of the power law slope α and the mean radius $\langle r \rangle$ as a function of f_{input}/f_{frag} . Error bars correspond to different noise realizations for the particles entering the system. Set of parameters as in Figure 1.

4. Discussion

We devised a fragmentation model based on the flow’s dynamical features (rate-of-strain tensor), particle size, and aging or degradation. This model does not intend to accurately replicate all the mechanisms of plastic fragmentation, but it does include some processes that lead to the observed size distribution. Specific characteristics of the different types of plastic (density, crystallinity, brittleness, etc.) or the presence of additives, which may influence the fragmentation, were not considered in this study. The parameter γ aims to account for the average characteristics of plastics and the effects of plastic weathering. The size distributions resulting from this model are congruent with observations in nature. The shear threshold dependency on the ratio r_0/r turns out to be critical for achieving this type of particle dispersion. Recently, George et al. (2024) [30] also introduced a threshold plastic length below which fragments will “almost never” break, resulting in the establishment of a PSD peak for intermediate-sized fragments. Aoki and Furue (2021) [31] introduced the concept of crush energy to account for the effect of the flow into the fragmentation process, considering that smaller pieces require larger energy.

The slope α of the power-law (1) and the mean radius of the steady size distribution were studied in relation to plastic aging, fragmentation rate, and primary particle release frequency rate. We showed that increasing particle degradation (or the amount of pieces a particle breaks into) promotes particle fragmentation of all sizes. However, increasing the fragmentation rate or decreasing the input of primary particles decreases the amount of bigger particles.

The fragmentation model should be extended to more complex three-dimensional physical models that account for the spatial and temporal variability of plastic transport in marine environments. While fragmentation may be the primary cause of the observed size distribution, other physical processes, such as vertical mixing, may have a size-dependent effect on plastic particles. Fragmented particles have different settling velocities, hence shear forces change with depth, influencing the critical threshold (2). Furthermore, the fate

of micro- and nano-sized particles is not correctly predicted in numerical hydrodynamic models, because their motion is regulated by sub-grid scale phenomena such as turbulence and collision, which are poorly understood and computationally expensive.

Supplementary Materials: The following supporting information can be downloaded at: <https://www.mdpi.com/article/10.3390/jmse12071213/s1>, Figure S1: Time evolution of the power-law slope $\alpha(t)$ (left panel) and the average size $\langle r(t) \rangle$ (right panel); Figure S2: Dependence of the power law slope α (left panel) and the mean radius $\langle r \rangle$ (right panel) as a function of the number of fragments N_{pieces} a particle splits into; Figure S3: Size distribution of plastic items found in the Mediterranean Sea during the MEDSEA campaign 2013 (blue dots), around the globe during the Malaspina circumnavigation in 2010 (black stars) and around the Balearic Islands (red squares).

Funding: We gratefully acknowledge financial support by FreeLitterAT Interreg Atlantic Project (EAPA-0009/2022) and Xunta de Galicia under Research Grant No. 2021-PG036-1. Financial support by the Galicia Marine Science programme included in the Recovery, Transformation and Resilience Plan (PRTR-C17.I1) is also acknowledged.

Institutional Review Board Statement: Not applicable.

Informed Consent Statement: Not applicable.

Data Availability Statement: The original contributions presented in the study are included in the article/Supplementary Materials, further inquiries can be directed to the corresponding author.

Conflicts of Interest: The authors declare no conflicts of interest.

Appendix A. Sinusoidal-Shear Flow Model

This is a simple demonstrative two-dimensional flow [35], displaying repeated stretching and folding and mimicking turbulent flow. In this flow, particles move in the domain $0 \leq x_i \leq L$, with periodic boundary conditions.

For the first half of the period ($nT \leq t < nT + T/2$), the particles move horizontally, with a velocity which depends on their vertical position. Specifically,

$$[u_1, u_2] = [V_{\max} \sin(2\pi x_2/L + \phi_n), 0] \quad (\text{A1})$$

During the second half of each period [$nT + T/2 \leq t < (n+1)T$], the particles move vertically, with a velocity that depends on their horizontal position,

$$[u_1, u_2] = [0, V_{\max} \sin(2\pi x_1/L + \phi_n)] \quad (\text{A2})$$

The constant V_{\max} sets the overall magnitude of the flow, and the phase ϕ_n is drawn randomly from the interval $[0, 2\pi)$ at the beginning of each half period.

References

1. Isobe, A.; Iwasaki, S. The fate of missing ocean plastics: Are they just a marine environmental problem? *Sci. Total Environ.* **2022**, *825*, 153935. [CrossRef]
2. Kaandorp, M.L.A.; Lobelle, D.; Kehl, C.; Dijkstra, H.A.; van Sebille, E. Global mass of buoyant marine plastics dominated by large long-lived debris. *Nat. Geosci.* **2023**, *16*, 689–694. [CrossRef]
3. Cole, M.; Lindeque, P.; Halsband, C.; Galloway, T.S. Microplastics as contaminants in the marine environment: A review. *Mar. Pollut. Bull.* **2011**, *62*, 2588–2597. [CrossRef] [PubMed]
4. Cózar, A.; Echevarría, F.; González-Gordillo, J.I.; Irigoien, X.; Úbeda, B.; Hernández-León, S.; Palma, Á.T.; Navarro, S.; de Lomas, J.G.; Ruiz, A.; et al. Plastic debris in the open ocean. *Proc. Natl. Acad. Sci. USA* **2014**, *111*, 10239–10244. [CrossRef]
5. van Sebille, E.; Aliani, S.; Law, K.L.; Maximenko, N.; Alsina, J.M.; Bagaev, A.; Bergmann, M.; Chapron, B.; Chubarenko, I.; Cózar, A.; et al. The physical oceanography of the transport of floating marine debris. *Environ. Res. Lett.* **2020**, *15*, 023003. [CrossRef]
6. George, M.; Fabre, P. Floating plastics in oceans: A matter of size. *Curr. Opin. Green Sustain. Chem.* **2021**, *32*, 100543. [CrossRef]
7. Kaandorp, M.L.A.; Dijkstra, H.A.; van Sebille, E. Modelling size distributions of marine plastics under the influence of continuous cascading fragmentation. *Environ. Res. Lett.* **2021**, *16*, 054075. [CrossRef]

8. Thompson, R.C.; Olsen, Y.; Mitchell, R.P.; Davis, A.; Rowland, S.J.; John, A.W.G.; McGonigle, D.; Russell, A.E. Lost at Sea: Where Is All the Plastic? *Science* **2004**, *304*, 838. [[CrossRef](#)] [[PubMed](#)]
9. Setälä, O.; Fleming-Lehtinen, V.; Lehtiniemi, M. Ingestion and transfer of microplastics in the planktonic food web. *Environ. Pollut.* **2014**, *185*, 77–83. [[CrossRef](#)]
10. Kooi, M.; Nes, E.H.v.; Scheffer, M.; Koelmans, A.A. Ups and Downs in the Ocean: Effects of Biofouling on Vertical Transport of Microplastics. *Environ. Sci. Technol.* **2017**, *51*, 7963–7971. [[CrossRef](#)]
11. Jalón-Rojas, I.; Wang, X.H.; Fredj, E. A 3D numerical model to track marine plastic debris (TrackMPD): Sensitivity of microplastic trajectories and fates to particle dynamical properties and physical processes. *Mar. Pollut. Bull.* **2019**, *141*, 256–272. [[CrossRef](#)]
12. Sutherland, B.R.; DiBenedetto, M.; Kaminski, A.; van den Bremer, T. Fluid dynamics challenges in predicting plastic pollution transport in the ocean: A perspective. *Phys. Rev. Fluids* **2023**, *8*, 070701. [[CrossRef](#)]
13. Cai, C.; Zhu, L.; Hong, B. A review of methods for modeling microplastic transport in the marine environments. *Mar. Pollut. Bull.* **2023**, *193*, 115136. [[CrossRef](#)] [[PubMed](#)]
14. Gilvarry, J. Fragment size in single fracture—A review of theory and experiment. *Wear* **1964**, *7*, 227–243. [[CrossRef](#)]
15. Oddershede, L.; Dimon, P.; Bohr, J. Self-organized criticality in fragmenting. *Phys. Rev. Lett.* **1993**, *71*, 3107–3110. [[CrossRef](#)] [[PubMed](#)]
16. Kadono, T. Fragment Mass Distribution of Platelike Objects. *Phys. Rev. Lett.* **1997**, *78*, 1444–1447. [[CrossRef](#)]
17. Kadono, T.; Arakawa, M. Crack propagation in thin glass plates caused by high velocity impact. *Phys. Rev. E* **2002**, *65*, 035107. [[CrossRef](#)]
18. Salman, A.; Biggs, C.; Fu, J.; Angyal, I.; Szabó, M.; Hounslow, M. An experimental investigation of particle fragmentation using single particle impact studies. *Powder Technol.* **2002**, *128*, 36–46. [[CrossRef](#)]
19. Timár, G.; Blömer, J.; Kun, F.; Herrmann, H.J. New Universality Class for the Fragmentation of Plastic Materials. *Phys. Rev. Lett.* **2010**, *104*, 095502. [[CrossRef](#)]
20. Brouzet, C.; Guiné, R.; Dalbe, M.J.; Favier, B.; Vandenberghe, N.; Villermaux, E.; Verhille, G. Laboratory model for plastic fragmentation in the turbulent ocean. *Phys. Rev. Fluids* **2021**, *6*, 024601. [[CrossRef](#)]
21. Wu, X.; Liu, P.; Shi, H.; Wang, H.; Huang, H.; Shi, Y.; Gao, S. Photo aging and fragmentation of polypropylene food packaging materials in artificial seawater. *Water Res.* **2021**, *188*, 116456. [[CrossRef](#)]
22. Chamas, A.; Moon, H.; Zheng, J.; Qiu, Y.; Tabassum, T.; Jang, J.H.; Abu-Omar, M.; Scott, S.L.; Suh, S. Degradation Rates of Plastics in the Environment. *ACS Sustain. Chem. Eng.* **2020**, *8*, 3494–3511. [[CrossRef](#)]
23. ter Halle, A.; Ladirat, L.; Gendre, X.; Goudouneche, D.; Pusineri, C.; Routaboul, C.; Tenailliau, C.; Duployer, B.; Perez, E. Understanding the Fragmentation Pattern of Marine Plastic Debris. *Environ. Sci. Technol.* **2016**, *50*, 5668–5675. [[CrossRef](#)] [[PubMed](#)]
24. Lindeque, P.K.; Cole, M.; Coppock, R.L.; Lewis, C.N.; Miller, R.Z.; Watts, A.J.; Wilson-McNeal, A.; Wright, S.L.; Galloway, T.S. Are we underestimating microplastic abundance in the marine environment? A comparison of microplastic capture with nets of different mesh-size. *Environ. Pollut.* **2020**, *265*, 114721. [[CrossRef](#)] [[PubMed](#)]
25. Lebreton, L.; Egger, M.; Slat, B. A global mass budget for positively buoyant macroplastic debris in the ocean. *Sci. Rep.* **2019**, *9*, 12922. [[CrossRef](#)] [[PubMed](#)]
26. Turcotte, D.L. Fractals and fragmentation. *J. Geophys. Res. Solid Earth* **1986**, *91*, 1921–1926. [[CrossRef](#)]
27. Åström, J.A. Statistical models of brittle fragmentation. *Adv. Phys.* **2006**, *55*, 247–278. [[CrossRef](#)]
28. Bird, N.R.A.; Watts, C.W.; Tarquis, A.M.; Whitmore, A.P. Modeling Dynamic Fragmentation of Soil. *Vadose Zone J.* **2009**, *8*, 197–201. [[CrossRef](#)]
29. Eriksen, M.; Lebreton, L.C.M.; Carson, H.S.; Thiel, M.; Moore, C.J.; Borerro, J.C.; Galgani, F.; Ryan, P.G.; Reisser, J. Plastic Pollution in the World's Oceans: More than 5 Trillion Plastic Pieces Weighing over 250,000 Tons Afloat at Sea. *PLoS ONE* **2014**, *9*, e111913. [[CrossRef](#)]
30. George, M.; Nallet, F.; Fabre, P. A threshold model of plastic waste fragmentation: New insights into the distribution of microplastics in the ocean and its evolution over time. *Mar. Pollut. Bull.* **2024**, *199*, 116012. [[CrossRef](#)]
31. Aoki, K.; Furue, R. A model for the size distribution of marine microplastics: A statistical mechanics approach. *PLoS ONE* **2021**, *16*, 1–19. [[CrossRef](#)] [[PubMed](#)]
32. Tsiaras, K.; Hatzonikolakis, Y.; Kalaroni, S.; Pollani, A.; Triantafyllou, G. Modeling the Pathways and Accumulation Patterns of Micro- and Macro-Plastics in the Mediterranean. *Front. Mar. Sci.* **2021**, *8*, 743117. [[CrossRef](#)]
33. Zahnw, J.C.; Vilela, R.D.; Feudel, U.; Tél, T. Aggregation and fragmentation dynamics of inertial particles in chaotic flows. *Phys. Rev. E* **2008**, *77*, 055301. [[CrossRef](#)] [[PubMed](#)]
34. Zahnw, J.C.; Maerz, J.; Feudel, U. Particle-based modeling of aggregation and fragmentation processes: Fractal-like aggregates. *Phys. D Nonlinear Phenom.* **2011**, *240*, 882–893. [[CrossRef](#)]
35. Neufeld, Z.; Hernández-García, E. *Chemical and Biological Processes in Fluid Flows: A Dynamical Systems Approach*; Imperial College Press: London, UK, 2010.
36. Spicer, P.T.; Pratsinis, S.E. Coagulation and fragmentation: Universal steady-state particle-size distribution. *AIChE J.* **1996**, *42*, 1612–1620. [[CrossRef](#)]
37. Virkar, Y.; Clauset, A. Power-law distributions in binned empirical data. *Ann. Appl. Stat.* **2014**, *8*, 89–119. [[CrossRef](#)]

38. Cózar, A.; Sanz-Martín, M.; Martí, E.; González-Gordillo, J.I.; Ubeda, B.; Gálvez, J.A.; Irigoien, X.; Duarte, C.M. Plastic Accumulation in the Mediterranean Sea. *PLoS ONE* **2015**, *10*, e0121762. [[CrossRef](#)]
39. Ruiz-Orejón, L.F.; Sardá, R.; Ramis-Pujol, J. Now, you see me: High concentrations of floating plastic debris in the coastal waters of the Balearic Islands (Spain). *Mar. Pollut. Bull.* **2018**, *133*, 636–646. [[CrossRef](#)]

Disclaimer/Publisher’s Note: The statements, opinions and data contained in all publications are solely those of the individual author(s) and contributor(s) and not of MDPI and/or the editor(s). MDPI and/or the editor(s) disclaim responsibility for any injury to people or property resulting from any ideas, methods, instructions or products referred to in the content.